Accurate Angle-of-Arrival Measurement Using Particle Swarm Optimization

Minghui Li, Kwok Shun Ho and Gordon Hayward

Department of Electronic and Electrical Engineering

The Centre for Ultrasonic Engineering (CUE)

University of Strathclyde, Royal College Building, 204 George Street

Glasgow, U.K., G1 1XW

Corresponding author:

Dr. David Minghui Li

Department of Electronic and Electrical Engineering

University of Strathclyde

Royal College Building

204 George Street

Glasgow G1 1XW

United Kingdom

E-mail: minghui.li@ieee.org

Accurate Angle-of-Arrival Measurement Using Particle Swarm Optimization

Minghui Li, Kwok Shun Ho and Gordon Hayward
Centre for Ultrasonic Engineering
University of Strathclyde, United Kingdom

ABSTRACT

As one of the major methods for location positioning, angle-of-arrival (AOA) estimation is a significant technology in radar, sonar, radio astronomy, and mobile communications. AOA measurements can be exploited to locate mobile units, enhance communication efficiency and network capacity, and support location-aided routing, dynamic network management, and many location-based services. In this paper, we propose an algorithm for AOA estimation in colored noise fields and harsh application scenarios. By modeling the unknown noise covariance as a linear combination of known weighting matrices, a maximum likelihood (ML) criterion is established, and a particle swarm optimization (PSO) paradigm is designed to optimize the cost function. Simulation results demonstrate that the paired estimator PSO-ML significantly outperforms other popular techniques and produces superior AOA estimates.

Keywords: array signal processing; angle-of-arrival (AOA) estimation; location positioning, particle swarm optimization; smart antennas

I. INTRODUCTION

Estimation of the incident signals' directions, or angle of arrival (AOA) estimation, is a fundamental problem in numerous applications such as radar, sonar, radio astronomy, and mobile communications. AOA measurements can locate mobile units, and thus support and enhance location-aided routing, dynamic network planning and management, and different types of location-based services and applications [1]; furthermore, it can improve communication efficiency and network capacity when integrated with adaptive array technology.

In general, location estimates of mobile units are derived from two types of measurements: AOA and range. The widely used range estimation models include received signal strength (RSS), time of arrival (TOA) and time difference of arrival (TDOA), where cooperation and synchronization between the transmitter and receiver are required [1]. On the contrary, the AOA model can locate targets in a non-cooperative, stealthy and passive manner, which is highly desirable in military and surveillance applications. The benefits of AOA measurements for location estimation have been widely investigated, and many AOA-alone [2]-[4] and hybrid systems [5]-[8] have been proposed.

A chief goal of wireless communication research has long been to enhance the network capacity, data rate and communication performance. In comparison with solutions of

increasing spectrum usage, smart antenna technology provides a more practical and cost-efficient solution. The benefits of using smart antennas are that the sender can focus the transmission energy towards the desired user while minimizing the effect of interference, and the receiver can form a directed beam towards the sender while simultaneously placing nulls in the directions of the other transmitters. This spatial filtering capability leads to increased user capacity, reduced power consumption, lower bit error rates (BER), and larger range coverage [9]-[10]. A key component that aids the array to be 'smart' and adaptive to the environment is AOA estimation of the desired signals and co-channel interferers. To fully exploit the AOA capability in mobile communications, various medium access control (MAC) protocols have been developed [11]-[13].

In recent years, AOA estimation has received considerable attention from radar and communication communities, and several high resolution algorithms have been proposed based on the white Gaussian noise model, such as multiple signal classification (MUSIC) [14], maximum likelihood (ML) [15], and others [16]-[17]. However, in many circumstances, the emitters reside in a "radio hostile" environment and the noise fields tend to be correlated along the array due to the dominant ambient noise [18]. Furthermore, the systems are often forced to work under unfavorable conditions involving low signal-to-noise ratio (SNR), highly correlated signals, and small array with few elements due to the cost, energy and size constraints. The standard AOA techniques become incompetent in such scenarios.

In this paper, we propose an algorithm for accurate AOA measurement in colored noise fields and harsh application scenarios. By modeling the unknown noise covariance as a linear combination of known weighting matrices, a maximum likelihood criterion is derived with respect to AOA and unknown noise parameters. ML criteria may yield superior statistical performance, but the cost function is multimodal, nonlinear and high-dimensional. To tackle it efficiently, we propose to use the particle swarm optimization (PSO) paradigm as a robust and fast global search tool. PSO is a recent addition to evolutionary algorithms first introduced by Eberhart and Kennedy [19]. Most of the applications demonstrated that PSO could give competitive or even better results in a much faster and cheaper way, compared to other heuristic methods such as genetic algorithms (GA) [20].

The PSO is designed to combine the problem-independent kernel and problem-specific features, which make the algorithm highly flexible while being specific and effective in the current application. Via extensive numerical studies, we demonstrate that the proposed algorithm yields superior performance over other popular methods, especially in unfavorable scenarios involving low SNR, highly correlated signals, short data samples, and small arrays.

The paper has been organized as follows. Section II describes mathematical models of the signal and noise, and derives the ML criterion function. In Section III, PSO-ML and the strategies for parameter selection are presented. Simulation results are given in Section IV, and Section V concludes the paper.

II. DATA MODEL AND PROBLEM FORMULATION

We consider an array of M elements arranged in an arbitrary geometry and N narrowband far-field sources at unknown locations. The complex M-vector of array outputs is modeled by the standard equation

$$\mathbf{y}(t) = \mathbf{A}(\boldsymbol{\theta})\mathbf{s}(t) + \mathbf{n}(t), \quad t = 1,\ 2,\ ...,\ L \tag{1}$$

where $\boldsymbol{\theta} = [\theta_1, \cdots, \theta_N]^T$ is the source AOA vector, and the *k*th column of the complex $M \times N$ matrix $\mathbf{A}(\boldsymbol{\theta})$ is the so called steering vector $\mathbf{a}(\theta_k)$ for the angle θ_k. The *i*th element $a_i(\theta_k)$ models the gain and phase adjustments of the *k*th signal at the *i*th element. Furthermore, the complex *N*-vector $\mathbf{s}(t)$ is composed of the emitter signals, and $\mathbf{n}(t)$ models the additive noise.

The vectors of signals and noise are assumed to be stationary, temporally white, zero-mean complex Gaussian random processes with second-order moments given by

$$\begin{aligned} E\left\{\mathbf{s}(t)\mathbf{s}^H(s)\right\} &= \mathbf{P}\delta_{ts} \\ E\left\{\mathbf{s}(t)\mathbf{s}^T(s)\right\} &= 0 \\ E\left\{\mathbf{n}(t)\mathbf{n}^H(s)\right\} &= \mathbf{Q}\delta_{ts} \\ E\left\{\mathbf{n}(t)\mathbf{n}^T(s)\right\} &= 0 \end{aligned} \tag{2}$$

where δ_{ts} is the Kronecker delta, $(\bullet)^H$ denotes complex conjugate transpose, $(\bullet)^T$ denotes transpose, and $E[\bullet]$ stands for expectation. Assuming that the noise and signals are independent, the data covariance matrix is given by

$$\mathbf{R} = E\left\{\mathbf{y}(t)\mathbf{y}^H(t)\right\} = \mathbf{A}\mathbf{P}\mathbf{A}^H + \mathbf{Q}. \tag{3}$$

Moreover, it is assumed that the number of sources is known or has been estimated using techniques, e.g., in [21]. The problem addressed herein is the estimation of $\boldsymbol{\theta}$ (and if necessary, along with the parameters in **P** and **Q**) from a batch of *L* measurements $\mathbf{y}(1)$, …, $\mathbf{y}(L)$.

Under the assumption of additive Gaussian noise and Gaussian distributed signals, the normalized (with *L*) negative log-likelihood function of the data vectors takes the form (ignoring the parameter independent terms) [22]

$$I(\boldsymbol{\theta}, \mathbf{P}, \mathbf{Q}) = \log|\mathbf{R}| + tr\left\{\mathbf{R}^{-1}\hat{\mathbf{R}}\right\}, \tag{4}$$

where $tr\{\bullet\}$ stands for trace, $\log|\bullet|$ denotes the natural logarithm of the determinant, and $\hat{\mathbf{R}}$ is the covariance matrix of the measured data

$$\hat{\mathbf{R}} = \frac{1}{L}\sum_{t=1}^{L}\mathbf{y}(t)\mathbf{y}^H(t). \tag{5}$$

In the follows, we focus on the ML criterion derived using parameterization of the noise covariance. Because this assumption applies no constraints to the signals, it is applicable to both cooperative and non-cooperative scenarios.

Based on a Fourier series expansion of the spatial noise power density function, the noise

covariance **Q** is assumed to be modeled by the following linear parameterization [18]:

$$\mathbf{Q}(\boldsymbol{\eta}) = \sum_{j=1}^{J} \eta_j \boldsymbol{\Sigma}_j \tag{6}$$

where $\boldsymbol{\eta} = [\eta_1, \cdots, \eta_J]^T$ is a vector of unknown noise Fourier coefficients, $\boldsymbol{\Sigma}_j$ is a known function of the array geometry given by

$$\boldsymbol{\Sigma}_j = \begin{cases} \bar{\boldsymbol{\Sigma}}_{(j-1)/2} & j \text{ odd} \\ \tilde{\boldsymbol{\Sigma}}_{j/2} & j \text{ even} \end{cases} \tag{7}$$

where

$$\begin{aligned} \bar{\boldsymbol{\Sigma}}_l &= \int_{-\pi}^{\pi} \mathbf{a}(\theta)\mathbf{a}^H(\theta)\cos(l\theta)d\theta \\ \tilde{\boldsymbol{\Sigma}}_l &= \int_{-\pi}^{\pi} \mathbf{a}(\theta)\mathbf{a}^H(\theta)\sin(l\theta)d\theta \end{aligned} \tag{8}$$

$l = 0,1,2,\cdots$. It is assumed that J is known or has been estimated [18], [21]. Similar descriptive models depicting the noise covariance as a linear combination of known weighting matrices are widely accepted in the literature [18], [21], [23], [29].

Following the derivation in [24], **P** can be solved in terms of $\mathbf{A}(\boldsymbol{\theta})$ and $\mathbf{Q}(\boldsymbol{\eta})$,

$$\hat{\mathbf{P}} = \left(\bar{\mathbf{A}}^H\bar{\mathbf{A}}\right)^{-1}\left[\bar{\mathbf{A}}^H\bar{\mathbf{R}}\bar{\mathbf{A}} - \bar{\mathbf{A}}^H\bar{\mathbf{A}}\right]\left(\bar{\mathbf{A}}^H\bar{\mathbf{A}}\right)^{-1}, \tag{9}$$

where

$$\begin{aligned} \bar{\mathbf{A}} &= \mathbf{Q}^{-1/2}\mathbf{A} \\ \bar{\mathbf{R}} &= \mathbf{Q}^{-1/2}\hat{\mathbf{R}}\mathbf{Q}^{-1/2}. \end{aligned} \tag{10}$$

By substituting (9) back to (3) and (4), the ML criterion function can be finally reduced to

$$I_1(\boldsymbol{\theta}, \boldsymbol{\eta}) = \log|\mathbf{Q}| + \log\left|\mathbf{G}\bar{\mathbf{R}}\mathbf{G} + \mathbf{H}\right| + tr\left\{\mathbf{H}\bar{\mathbf{R}}\right\}, \tag{11}$$

where

$$\begin{aligned} \mathbf{G} &= \bar{\mathbf{A}}\left(\bar{\mathbf{A}}^H\bar{\mathbf{A}}\right)^{-1}\bar{\mathbf{A}}^H \\ \mathbf{H} &= \mathbf{I} - \mathbf{G}. \end{aligned} \tag{12}$$

The ML estimates of $\boldsymbol{\theta}$ and $\boldsymbol{\eta}$ are obtained by minimizing (11). Based on the data model, the Cramer-Rao bound (CRB) for AOA estimation can be derived [18],

$$\mathrm{CRB}(\boldsymbol{\theta}) = \frac{1}{2L}\left[\mathrm{Re}\left\{\left(\mathbf{P}\mathbf{A}^H\mathbf{R}^{-1}\mathbf{A}\mathbf{P}\right)\odot\left(\mathbf{D}^H\mathbf{R}^{-1}\mathbf{D}\right)^T + \left(\mathbf{P}\mathbf{A}^H\mathbf{R}^{-1}\mathbf{D}\right)\odot\left(\mathbf{P}\mathbf{A}^H\mathbf{R}^{-1}\mathbf{D}\right)^T\right\}\right]^{-1}, \tag{13}$$

where $\mathrm{Re}[\bullet]$ represents the real part, $\odot$ denotes element-wise product, and

$$\mathbf{D} = \left[\left.\frac{\partial\mathbf{a}(\theta)}{\partial\theta}\right|_{\theta=\theta_1} \cdots \left.\frac{\partial\mathbf{a}(\theta)}{\partial\theta}\right|_{\theta=\theta_N}\right]. \tag{14}$$

III. PSO-ML AOA ESTIMATION AND PARAMETER SELECTION

Particle swarm optimization is a stochastic optimization paradigm, which mimics animal social behaviors such as flocking of birds and the methods by which they find roosting places or food sources [19]. PSO starts with the initialization of a population of individuals in the search space and works on the social behavior of the particles in the swarm. Each particle is assigned a position in the problem space, which represents a candidate solution to the problem under consideration. Each of these particle positions is scored to obtain a scalar cost, named fitness, based on how well it solves the problem. These particles then fly through the problem space subject to both deterministic and stochastic update rules to new positions, which are subsequently scored. Each particle adaptively updates its velocity and position according to its own flying experience and its companions' flying experience, aiming at a better position for itself. As the particles traverse the search space, each particle remember its own personal best position that it has ever visited, and it also knows the best position found by any particle in the swarm. On successive iterations, each particle takes the path of a damped oscillatory movement towards its personal best and the global best positions. With the oscillation and stochastic adjustment, particles explore regions throughout the problem space and eventually settle down near a good solution.

As illustrated in Fig. 1, the algorithm starts by initializing a population of particles in the "normalized" search space with random positions **x** and random velocities **v**, which are constrained between zero and one in each dimension. The position vector of the *i*th particle takes the form $\mathbf{x}_i = \left[\tilde{\theta}_1, \cdots \tilde{\theta}_N, \tilde{\eta}_1, \cdots, \tilde{\eta}_J\right]$, where $0 \le \tilde{\theta}_n, \tilde{\eta}_j < 1$, $n = 1, \cdots, N$, $j = 1, \cdots, J$, $N \ge 1$, $J \ge 1$. A particle position vector is converted to a candidate solution vector in the problem space through a mapping. The score of the mapped vector evaluated by the likelihood function $I_1(\boldsymbol{\theta}, \boldsymbol{\eta})$ (11) is regarded as the fitness of the corresponding particle.

Fig. 1. Flowchart illustrating main steps of PSO-ML technique.

The *i*th particle's velocity is updated according to (15)

$$\mathbf{v}_i^{k+1} = \omega^k \mathbf{v}_i^k + c_1 \mathbf{r}_1^k \odot \left(\mathbf{p}_i^k - \mathbf{x}_i^k\right) + c_2 \mathbf{r}_2^k \odot \left(\mathbf{p}_g^k - \mathbf{x}_i^k\right), \tag{15}$$

where $\mathbf{p}_i$ is the best previous position of the *i*th particle, $\mathbf{p}_g$ is the best position found by any particle in the swarm, $k = 1, 2, \ldots$, indicates the iterations, ω is a parameter called the inertia weight, c_1 and c_2 are positive constants referred to as cognitive and social parameters respectively, $\mathbf{r}_1$ and $\mathbf{r}_2$ are independent random vectors.

Three components typically contribute to the new velocity. The first part refers to the inertial effect of the movement. The inertial weight ω is considered critical for the convergence behavior of PSO [25]. A larger ω facilitates searching new area and global exploration while a smaller ω tends to facilitate fine exploitation in the current search area. In this study, ω is selected to decrease during the optimization process, thus PSO tends to have more global search ability at the beginning while having more local search ability near the

end. Given a maximum value $\omega_{\max}$ and a minimum value $\omega_{\min}$, ω is updated as follows:

$$\omega^k = \begin{cases} \omega_{\max} - \dfrac{\omega_{\max} - \omega_{\min}}{rK}(k-1), & 1 \le k \le \lceil rK \rceil \\ \omega_{\min}, & \lceil rK \rceil + 1 \le k \le K \end{cases} \tag{16}$$

where $[rK]$ is the number of iterations with time decreasing inertial weights, $0 < r < 1$ is a ratio, and K is the maximum iteration number. Based on empirical practice and extensive test runs, we select $\omega_{\max} = 0.9$, $\omega_{\min} = 0.4$, and $r = 0.4 \sim 0.8$. The second and third components introduce stochastic tendencies to return towards the particle's own best historical position and the group's best historical position. Constants c_1 and c_2 are used to bias the particle's search towards the two locations. Following common practice in the literature [26], c_1=c_2=2, although these values could be fine-turned for the problem at hand.

Since there was no actual mechanism for controlling the velocity of a particle, it is necessary to define a maximum velocity to avoid the danger of swarm explosion and divergence [27]. The velocity limit is applied to $\mathbf{v}_i$ along each dimension separately by

$$v_{id} = \begin{cases} V_{MAX}, & v_{id} > V_{MAX} \\ -V_{MAX}, & v_{id} < -V_{MAX} \end{cases} \tag{17}$$

where d=1,…, N+J. Like the inertial weight, large values of V_{MAX} encourage global search while small values enhance local search. In this study, V_{MAX} is held constant at 0.5, the half dynamic range, throughout the optimization.

The new particle position is calculated using (18),

$$\mathbf{x}_i^{k+1} = \mathbf{x}_i^k + \mathbf{v}_i^{k+1}. \tag{18}$$

If any dimension of the new position vector is less than zero or greater than one, it is clipped to stay within this range. It should be noted that, at any time of the optimization process, two components representing AOA in a position vector are not allowed to be equal.

The final global best position $\mathbf{p}_g$ is taken as the ML estimates of AOA and noise parameters. Some previous works demonstrate that the performance of PSO is not significantly affected by changing the swarm size P. The typical range of P is 20 to 50, which is sufficient for most problems to achieve good results [28]. In addition, PSO is robust to control parameters; and the convergence and stability analysis is presented in [27].

IV. SIMULATION RESULTS

Two examples are presented to evaluate PSO-ML against the least square estimator (LSE) [29], MUSIC [14], and the unconditional maximum likelihood (UML) method [15]. LSE is a superior direction finding technique in colored noise fields established based on a similar noise model, MUSIC is one of the most popular techniques, and UML represents the best estimator under white Gaussian noise assumption [30].

The selected PSO parameters are summarized in Table 1. The PSO algorithm starts with random initialization, and is terminated if the maximum iteration number K is reached or the global best particle position is not updated in 20 successive iterations. We have performed

300 Monte Carlo experiments for each point of the plot.

Table 1 Selected PSO parameters

A. Example 1

Assume that two equal-power correlated signals with the correlation factor r=0.95, impinge on a four-element uniform linear array (ULA) from 90° and 95°. The number of snapshots is 80. The situation is challenging, since the separation of emitters is about 0.19 beamwidth, the conventional resolution limit. The noise covariance is modeled as a linear combination of known matrices (6), J=3, and $\boldsymbol{\eta} = [1, 1/4, 1/9]$. Similar noise models are used in the literature [29]. Fig. 2 depicts the combined AOA estimation root-mean-squared errors (RMSE) obtained using PSO-ML, LSE, MUSIC and UML as a function of SNR, and compares them with the corresponding CRB (13) (theoretically best performance). Fig. 3 shows the resolution probabilities for the same methods. Two sources are considered to be resolved in an experiment if both estimation errors are less than the half of their angular separation.

As can be seen from Fig. 2 and Fig. 3, PSO-ML yields significantly superior performance over LSE, MUSIC and UML as a whole, by demonstrating lower estimation RMSE and higher resolution probabilities. PSO-ML produces excellent AOA estimates with RMSE approaching and asymptotically attaining the theoretic lower bound. On the other hand, as a standard high-resolution method, MUSIC fails almost in the whole SNR range. Although UML is an optimal technique in white Gaussian noise, it completely fails when SNR is lower than 15dB and only produces acceptable estimates in high SNR region. It is worth noting that the advantages of PSO-ML over the other methods are more prominent when SNR is low, and the benefits can be extended to other unfavorable conditions.

Fig. 2 AOA estimation RMSE of PSO-ML, LSE, MUSIC and UML versus SNR. Dashdot line represents theoretic CRB. Two correlated sources impinge on four-element ULA at 90° and 95°, r=0.95. Number of snapshots is 80.

Fig. 3 Resolution probabilities of PSO-ML, LSE, MUSIC and UML versus SNR. Two correlated sources impinge on four-element ULA at 90° and 95°, r=0.95. Number of snapshots is 80.

B. Example 2

In the second example, we consider an 8-element ULA. Two emitters are present at 80° and 83° with a separation of 0.23 beamwidth, r=0.9. The number of snapshots is 30. In the noise model (6), J=5 and $\boldsymbol{\eta} = [1, 0.75, 0.5, 0.25, 0.1]$. Fig. 4 illustrates the RMSE values obtained from PSO-ML, LSE, MUSIC and UML. The resolution probabilities for the same methods are shown in Fig. 5.

As expected, PSO-ML significantly outperforms LSE, MUSIC and UML and produces more accurate estimates by showing lower RMSE and higher resolution probabilities. We

select a different scenario in this example, although the source separation in terms of array beamwidth is similar, the data sample is much shorter and there is more freedom in the noise model as compared with Example 1. As shown in Fig. 2 - Fig. 5, the benefits of PSO-ML over LSE with colored noise model and UML and MUSIC under white Gaussian noise assumption appear to be more prominent in unfavorable scenarios involving low SNR, short data samples, closely spaced and highly correlated sources, and unknown noise environment.

Fig. 4. AOA estimation RMSE of PSO-ML, LSE, MUSIC and UML versus SNR. Dashdot line represents theoretic CRB. Two correlated sources impinge on eight-element ULA at 80° and 83°, r=0.9. Number of snapshots is 30.

Fig. 5. Resolution probabilities of PSO-ML, LSE, MUSIC and UML versus SNR. Two correlated sources impinge on eight-element ULA at 80° and 83°, r=0.9. Number of snapshots is 30.

V. CONCLUSIONS

Arising from the requirements of radio localization, efficient communication by directional transmission and interference suppression, and exploration of angular diversity for various benefits such as location-aided routing and network management, AOA measurement is an important technology of growing practical interest in numerous applications such as radar, radio astronomy, and mobile communications. In this paper, we propose an algorithm for AOA estimation in colored noise fields and unfavorable application scenarios based on the maximum likelihood principle and implemented using the PSO paradigm. Simulation results demonstrate that PSO-ML significantly outperforms other popular techniques and produces more accurate AOA estimates, especially in unfavorable scenarios.

REFERENCES

[1] G. Mao, B. Fidan, and B. Anderson, "Wireless sensor network localization techniques," *Computer Networks*, vol. 51, pp. 2529-2553, Jan. 2007.

[2] D. Niculescu and B. Nath, "Ad hoc positioning system (APS) using AOA," in *Proc. IEEE INFOCOM 2003*, San Francisco, pp. 1734-1743, Mar. 2003.

[3] M. Gavish and A. Weiss, "Performance analysis of bearing-only target location algorithms," *IEEE Trans. Aerosp. Electron. Syst.*, vol. 28, pp. 817-828, July 1992.

[4] T. Biedka, J. Reed, and B. Woerner, "Direction finding methods for CDMA systems," in *Proc. 13th Asilomar Conference on Signals, Systems and Computers*, pp. 637-641, Nov. 1996.

[5] Z. Gu and E. Gunawan, "Radiolocation in CDMA cellular system based on joint angle and delay estimation," *Wireless Personal Communications*, vol. 23, pp. 297-309, July 2002.

[6] L. Cong and W. Zhuang, "Hybrid TDOA/AOA mobile user location for wideband CDMA cellular systems," *IEEE Trans. on Wireless Commun.*, vol. 1, pp. 439-447, July 2002.

[7] J. Ash and L. Potter, "Sensor network localization via received signal strength measurements with directional antennas," in *Proc. 42nd Annual Allenton Conference on Communication, Control, and Computing*, Champaign-Urbana, IL, pp. 1861-1870, Sept. 2004.

[8] T. Chen, C. Chiu, and T. Tu, "Mixing and combining with AOA and TOA for the enhanced accuracy of mobile location," in *Proc. 5th European Personal Mobile Communications Conference*, Glasgow, UK, pp. 276-280, Apr. 2003.

[9] M. H. Li, Y. L. Lu, H.-H. Chen, B. Wang, and I-M. Chen, "Angle of Arrival (AOA) Estimation in Wireless Networks," in J. Feng (Eds.), *Wireless Networks – Research, Technology and Applications*, Chapter 5, Nova Science Publishers, Inc. New York, 2009, pp. 135-164.

[10] J. Liberti and T. Rappaport, *Smart Antennas for Wireless Communications*, Prentice Hall, 1999.

[11] S. Bellofiore, J. Foutz, R. Govindarajula, I. Bahceci, C. Balanis, A. Spanias, J. Capone, and T. Duman, "Smart antenna system analysis, integration, and performance for mobile ad-hoc networks (MANETs)," *IEEE Trans. Antennas Propagat.*, vol. 50, pp. 571-581, May 2002.

[12] H. Koubaa, "Reflections on smart antennas for MAC protocols in multihop ad hoc networks," in *Proc. European Wireless'02*, pp. 25-28, Feb. 2002.

[13] H. Singh and S. Singh, "Tone based MAC protocol for use with adaptive array antennas," in *Proc. IEEE WCNC 2004*, pp. 1246-1251, Mar. 2004.

[14] R. Schmidt, "Multiple emitter location and signal parameter estimation," *IEEE Trans. Antennas Propagat.*, vol. 34, pp. 276-280, Mar. 1986.

[15] M. H. Li and Y. L. Lu, "A refined genetic algorithm for accurate and reliable DOA estimation with a sensor array," *Wireless Personal Communications*, vol. 43, pp. 533-547, Oct. 2007.

[16] M. H. Li and Y. L. Lu, "Improving the performance of GA-ML DOA estimator with a resampling scheme," *Signal Processing*, vol. 84, pp. 1813-1822, Oct. 2004.

[17] M. H. Li and Y. L. Lu, "Dimension reduction for array processing with robust interference cancellation," *IEEE Trans. Aerosp. Electron. Syst.*, vol. 42, pp.103-112, Jan. 2006.

[18] M. H. Li and Y. L. Lu, "Angle-of-arrival estimation for localization and communication in wireless networks," in *Proc. 16th European Signal Processing Conference (EUSIPCO 2008)*, Lausanne, Switzerland, Aug. 2008.

[19] R. C. Eberhart and J. Kennedy, "A new optimizer using particle swarm theory," in *Proc. 6th Symp. Micro Machine and Human Science*, Nagoya, Japan, pp. 39-43, 1995.

[20] M. H. Li and Y. L. Lu, "Source bearing and steering-vector estimation using partially calibrated arrays," *IEEE Trans. Aerosp. Electron. Syst.*, vol. 45, pp.1361-1372, Oct. 2009.

[21] J.-J. Fuchs, "Estimation of the number of signals in the presence of unknown correlated sensor noise," *IEEE Trans. Signal Processing*, vol. 40, pp. 1053-1061, May 1992.

[22] B. Ottersten, M. Viberg, P. Stoica, and A Nehorai, "Exact and large sample maximum likelihood techniques," *Radar Array Processing*, S. Haykin, J. Litva and T. J. Shepherd, Eds. New York: Springer-Verlag, pp. 99-152, Jan 1993.

[23] F. Vanpoucke and A. Paulraj, "A harmonic noise model for direction finding in colored ambient noise," *IEEE Signal Processing Letters*, vol. 2, pp. 135-137, July 1995.

[24] A. G. Jaffer, "Maximum likelihood direction finding of stochastic sources: A separable solution," in *Proc. ICASSP-88*, New York, NY, Apr. 1988, pp. 2893-2896.

[25] K. E. Parsopoulos and M. N. Vrahatis, "Recent approaches to global optimization problems through particle swarm optimization," *Natural Computing*, vol. 1, pp. 235-306, 2002.

[26] R. C. Eberhart and Y. Shi, "Particle swarm optimization: Developments, applications and resources," in *Proc. 2001 Congress on Evolutionary Computation (CEC2001)*, Seoul, Korea, pp. 81-86, May 2001.

[27] M. Clerc and J. Kennedy, "The particle swarm-explosion, stability, and convergence in a multidimensional complex space," *IEEE Trans. Evol. Comput.*, vol. 6, pp.58-73, Feb. 2002.

[28] R. C. Eberhart and Y. Shi, "Comparing inertia weights and constriction factors in particle swarm optimization," in *Proc. 2000 Congress on Evolutionary Computation (CEC2000)*, San Diego, CA, pp. 84-88, July 2000.

[29] J. F. Böhme and D. Kraus, "On least squares methods for direction of arrival estimation in the presence of unknown noise fields," in *Proc. ICASSP-88*, New York, NY, Apr. 1988, pp. 2833-2836.

[30] P. Stoica and A. Nehorai, "Performance study of conditional and unconditional direction-of-arrival estimation," *IEEE Trans. Acoust., Speech, Signal Processing*, vol. 38, pp. 1783-1795, Oct. 1990.

Table 1 Selected PSO parameters

Parameter	Value
c_1	2.0
c_2	2.0
P	20
K	200
V_{MAX}	0.5
$\omega_{\max}$	0.9
$\omega_{\min}$	0.4
r	0.5

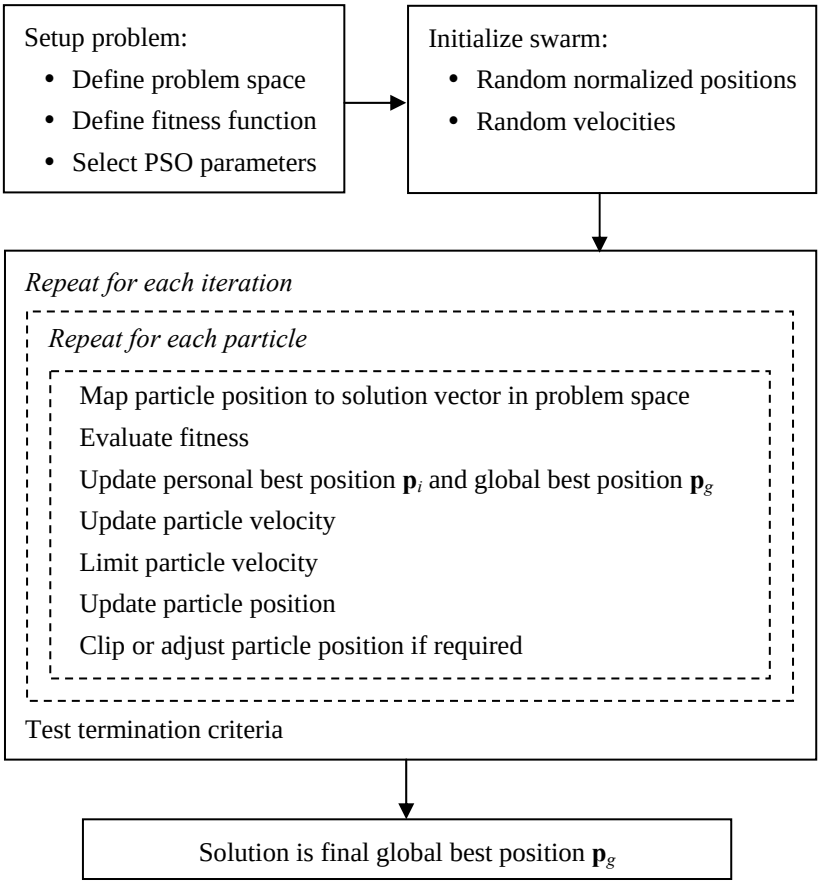

Fig. 1. Flowchart illustrating main steps of PSO-ML technique.

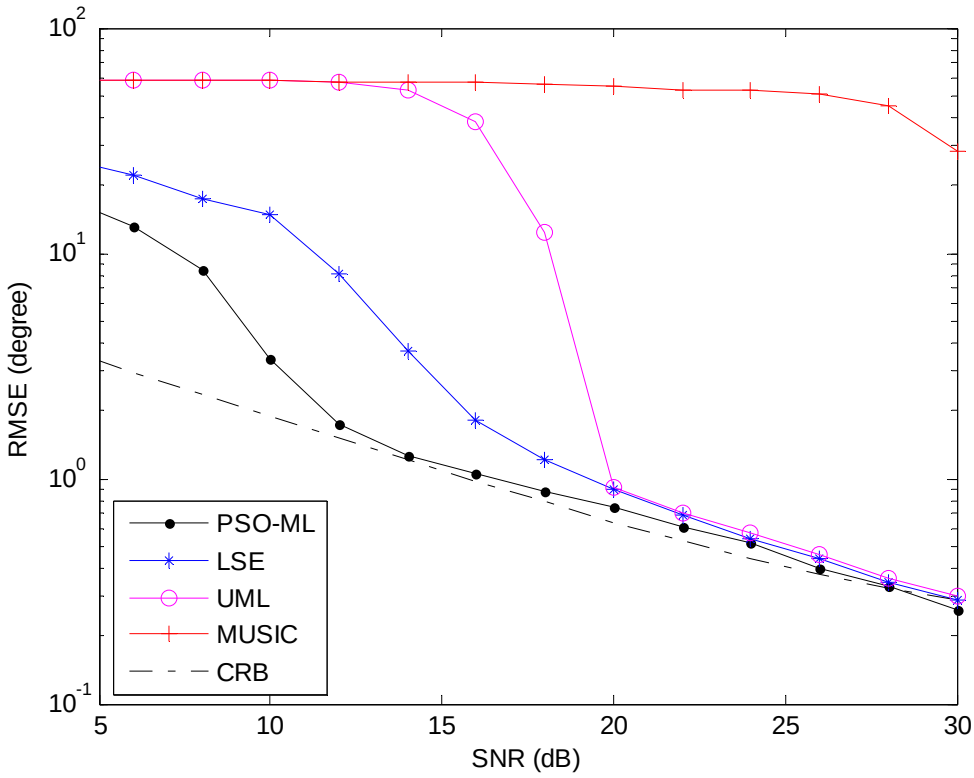

Fig. 2 AOA estimation RMSE of PSO-ML, LSE, MUSIC and UML versus SNR. Dashdot line represents theoretic CRB. Two correlated sources impinge on four-element ULA at 90° and 95°, r=0.95. Number of snapshots is 80.

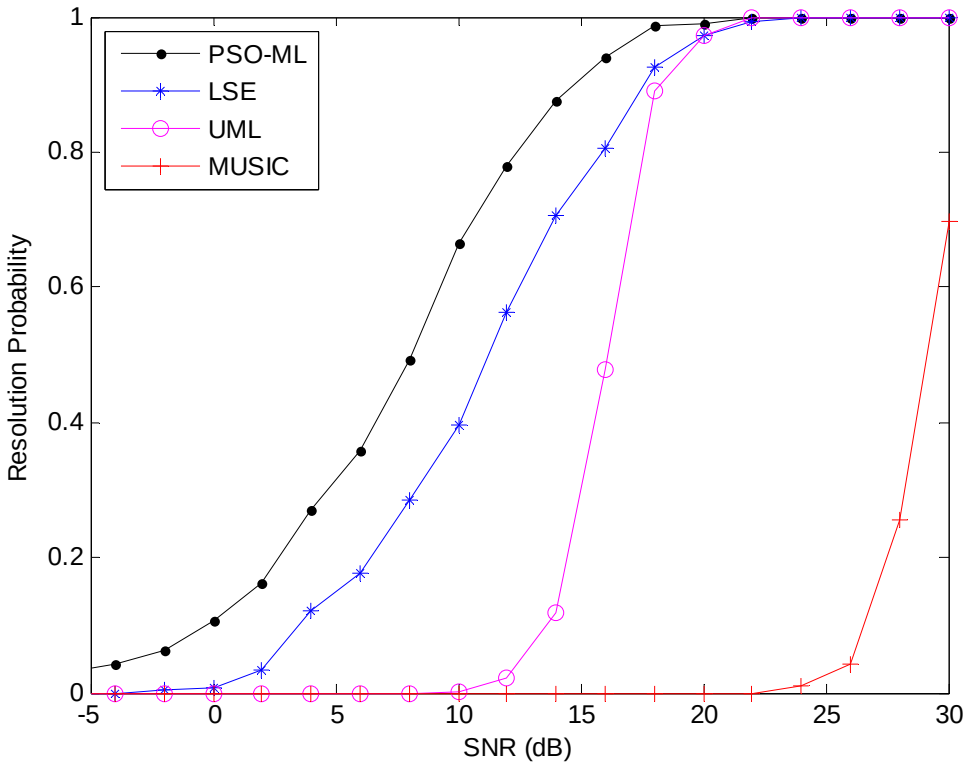

Fig. 3 Resolution probabilities of PSO-ML, LSE, MUSIC and UML versus SNR. Two correlated sources impinge on four-element ULA at 90° and 95°, r=0.95. Number of snapshots is 80.

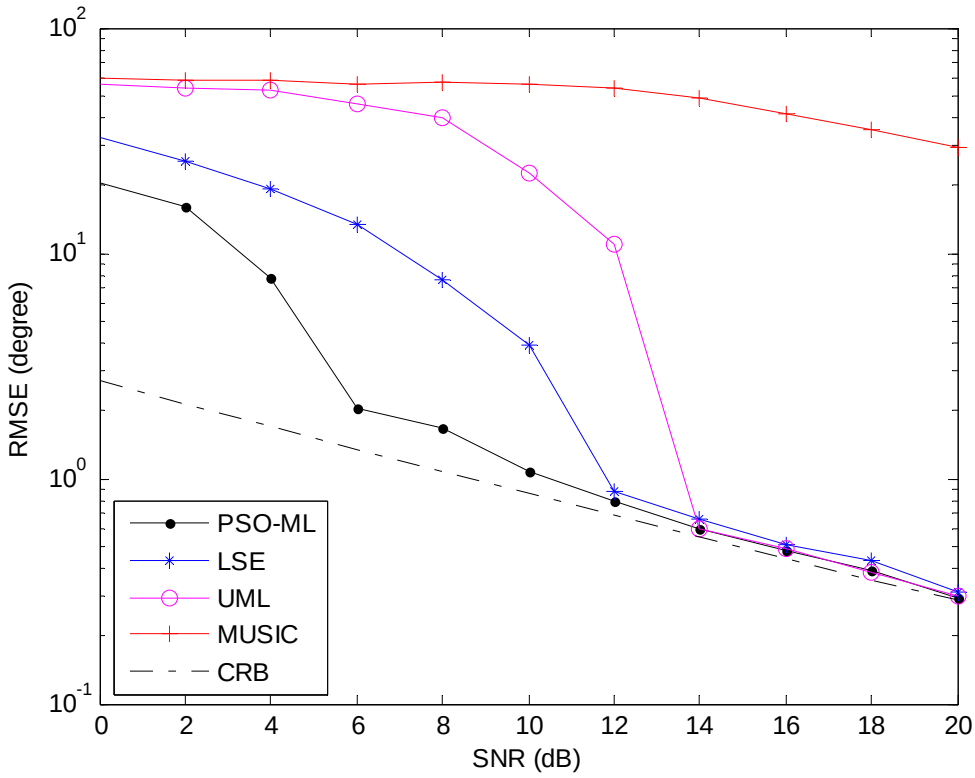

Fig. 4. AOA estimation RMSE of PSO-ML, LSE, MUSIC and UML versus SNR. Dashdot line represents theoretic CRB. Two correlated sources impinge on eight-element ULA at 80° and 83°, r=0.9. Number of snapshots is 30.

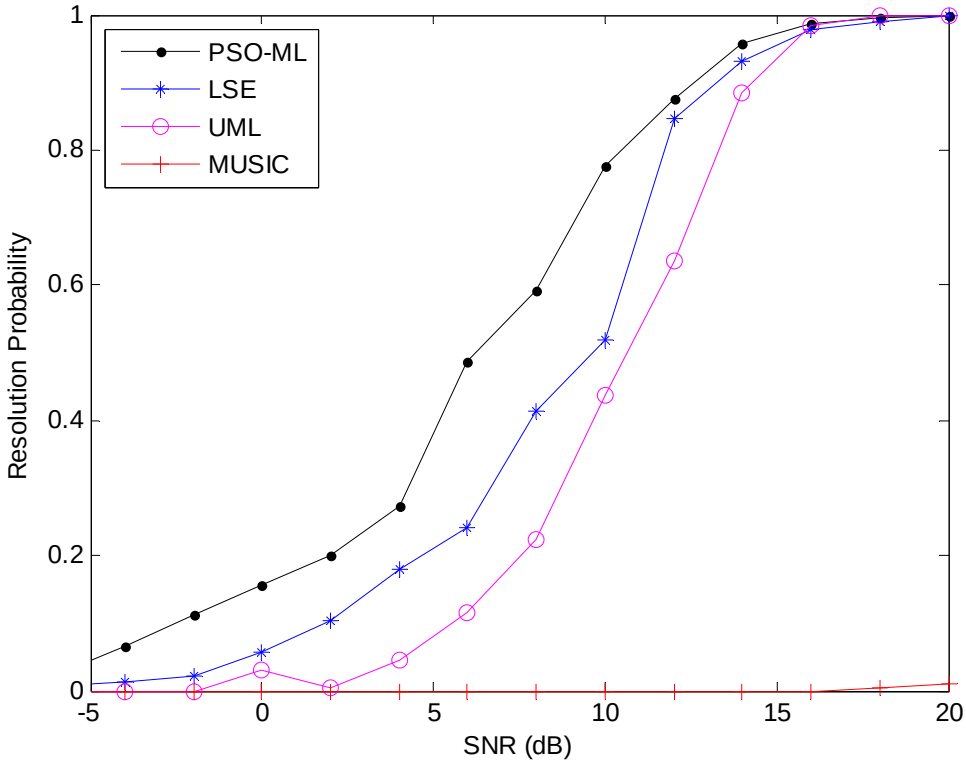

Fig. 5. Resolution probabilities of PSO-ML, LSE, MUSIC and UML versus SNR. Two correlated sources impinge on eight-element ULA at 80° and 83°, r=0.9. Number of snapshots is 30.